Hydrogen effect on zirconium alloy surface treated by pulsed electron beam

N.S. Pushilina [a], A.M. Lider [a], V.N. Kudiiarov [a,*], I.P. Chernov [a], S.V. Ivanova [b]

[a] Department of General Physics, Institute of Physics and Technology, National Research Tomsk Polytechnic University, Lenin Avenue 30, Tomsk 634050, Russia
[b] National Research Nuclear University "MIFI", Kashirskoye shosse 31, Moscow 115409, Russia

ABSTRACT

Influence of modification by pulsed electron beam (PEB) and hydrogen adsorption in zirconium alloys have been investigated. Treatment of Zr–1Nb alloy by high-current PEB allows for a decrease in the amount of hydrogen absorbed by the samples during the hydrogenation process from gas atmosphere in the temperature range of (350–550 °C). The effect of the PEB surface treatment on the hydrogen adsorption connected with the formation of a protective oxide film after PEB irradiation and also by the formation of a specific hardening structure under the action of irradiation at temperatures exceeding the melting temperature from the subsequent high-speed surface cooling.

1. Introduction

Zirconium alloys are the construction materials for critical elements in active zones of nuclear power reactors. During the operation of reactors such materials are subject to hydrogenation [1–3]. The Technical conditions of operation do not prevent hydrogen infiltration into components made of zirconium alloys [4]. The sources of hydrogen accumulation in the components are hydrogen: hydrogen during the corrosion reaction with the coolant and also hydrogen that is present within the fuel cladding that emanates from the fuel during the operation. The amount of accumulated hydrogen depends on a number of factors: surface quality, alloying components, operation temperature, corrosion rate, and etc. Hydrogenation results in a decrease of alloy plasticity and cracking resistance. In addition, the formation of brittle hydrides at crack tips can result in severe embrittlement. Consequently, one of the most important requirements for the reactor's active zone materials is low hydrogen absorptivity. Thus, the protection of metal constructions subject to hydrogen exposure in hydrogen-containing environments is of vital importance.

Recently, among a number of methods developed for surface treatment and creation of protective coatings [5–14]. In particular, the application of pulsed electron beams (PEB) results in increased hardness, corrosion, wear resistance and lowers the friction coefficient of construction materials. For instance, authors of [5–7] have shown that irradiation by three electron beam pulses with a duration of 50 μs and an energy density of 18 J/cm^2 results in an increase of micro- and nanohardness of Zr–1Nb alloy of up to 40%. The calculation of temperature profiles has shown that by the end of the pulse the thickness of the melted layer amounted to about 8 μm and the heat-affected zone was about 20 μm. We have established that the treatment of zirconium alloys results in a significant decrease (2–3 times) of hydrogen that infiltrates into the alloy in comparison with untreated samples. The mechanism by which hydrogen adsorption is reduced for zirconium alloys after treatment by pulsed electron beam is still undiscovered. The considered aspects prompt a complex investigation of hydrogen interaction with zirconium alloys after PEB treatment.

2. Materials and research methods

Materials used in this research were zirconium alloy Zr–1Nb samples with dimensions of 50 × 50 × 0.7 mm. The samples were irradiated by pulsed electron beams using a "Solo" device in Institute of High Current Electronics of Siberian Branch of the Russian Academy Of Science. The both sides of each sample were treated with an energy density of 18 J/cm^2. Every sample was irradiated by three pulses for a duration of 50 μs. The analysis of the alloy surface structure was performed by transmission electron microscopy. The structure and phase composition was analyzed using a Shimadzu XRD 6000 diffractometer. The samples were saturated with hydrogen using a PCI «Gas Reaction Controller» [15] device. The hydrogen concentration was determined by a RHEN602 LECO device using the principle of melting in an inert atmosphere. The amount of released hydrogen is measured in a thermal conductivity cell.

* Corresponding author. Tel.: +7 9138700989.
  E-mail address: viktor.kudiiarov@gmail.com (V.N. Kudiiarov).

Investigation of the elemental depth distribution was performed using an optical radio frequency glowing discharge spectrometer, GD-OES Profiler2, produced by the Horiba company. Incident particles (argon atoms) with energies less than 50 eV impinge on the surface at a wide incident angle, which creates uniform sputtering without deformation of the surface. The obvious advantages of optical emission spectrometry are: speed, low analysis cost, and a well-proven procedure of automated sample preparation. In comparison with the secondary ion mass spectrometry method, which is also used for isotopic analysis, the optical emission spectrometry allows one to obtain equivalent results in minutes compared to hours for the SIMS [16]. The investigation was performed at a working gas pressure of 650 Pa.

3. Results

3.1. Effect of pulsed electron beam treatment on properties of zirconium alloy Zr–1Nb

Fig. 1 depicts the images of a zirconium alloy surface in its initial state and after pulsed beam treatment. Irradiation by pulsed electron beams and the consequent recrystallization of the zirconium alloy results in the formation of a micro structure with thin (needle-shaped) plates that dissect the grains.

Significant changes in the microstructure of the modified samples were caused by high heating and cooling rates of the material during PEB. As a result of high-speed cooling (10^7–10^8 K/s) in the surface layer of the alloy (less than 8 μm) the formation of martensite with a complicated morphology. The detailed investigation of the surface structure with TEM has shown that martensite plates fill the grains entirely (Fig. 2).

The martensitic plate sizes varied from 0.1 to 0.3 μm (mainly 0.1 μm). The martensite plates also contained nanoparticle aggregates with sizes of 15 nm. Twins were also present in the form of parallel in plates (Fig. 2a). The width of twin layers ranges from 60 to 170 nm.

X-ray structural analysis confirms and supplements the results of electron microscopic analysis. The pulsed electron beams leads to an evident change in the structure phase state of the material. The decrease in zirconium lattice parameters after irradiation is related to the formation of martensite phase α′-Zr. A further investigation of the depth distribution of Zr, O, H showed that the irradiation resulted in an increase of oxygen concentration and growth of the oxide layer in each sample (Fig. 3). However, the hydrogen content in the Zr–1Nb alloy before and after the treatment is almost constant.

According to the results of hydrogen concentration measurements, the hydrogen content in the initial sample was 0.032 ± 0.003 at.%. After the PEB irradiation the content amounted to 0.056 ± 0.006 at.%.
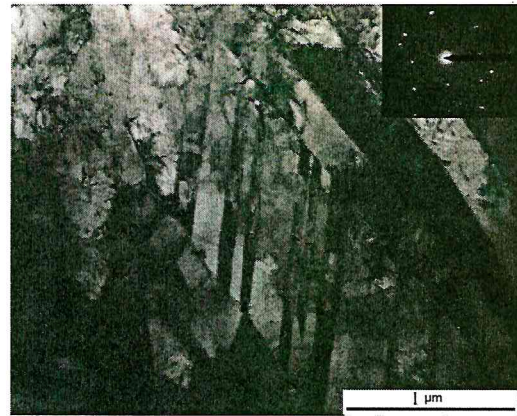

Fig. 2. TEM of the irradiated Zr–1Nb alloy surface.

3.2. Adsorption and distribution of hydrogen

The next stage included the hydrogen adsorption investigation by the zirconium alloys that had been subject to different surface treatment method. Figs. 4 and 5 represent isotherms of Zr–1Nb alloy interaction with hydrogen. The hydrogen concentration was determined by manometric method [17].

4. Discussion

With the help of XRD analysis data and the structural diagram of the Zr–H system [16], the results were interpreted in the following way. One can see that before the saturation of the α-phase with hydrogen there is a linear dependence of hydrogen adsorption rate vs. hydrogenation time. There are changes in slope on the sorption curves that caused by the change of hydrogen diffusion rate in the material due to phase transitions. For instance, at the saturation temperature of 450 °C the sorption rate change is caused by α → (α + δ) → δ transitions. If the hydrogenation time is increased further, the hydrogen diffusion rate is significantly decreased. These results conform well with the theory, since the hydrogen diffusion in the hydride phase is known to be two orders of magnitude lower – than the diffusion in α and β phases of zirconium. Another tendency is attributed to the fact that a zirconium hydride lattice containing more than 46.3 at.% of hydrogen at such temperatures becomes thermodynamically unstable and tends to change composition. At 550 °C the first inflexion point is observed at hydrogen concentrations of about 24.7 at.%, which matches the phase transition of (α + δ) into the phase β. The next stage is a saturation of the β phase with hydrogen. During the hydrogen saturation of the PEB treated samples at the temperature range
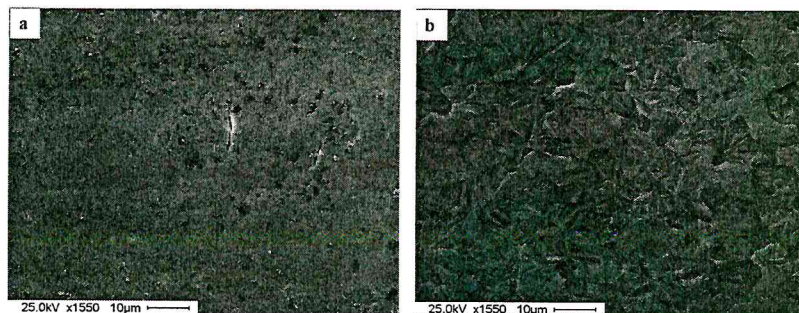

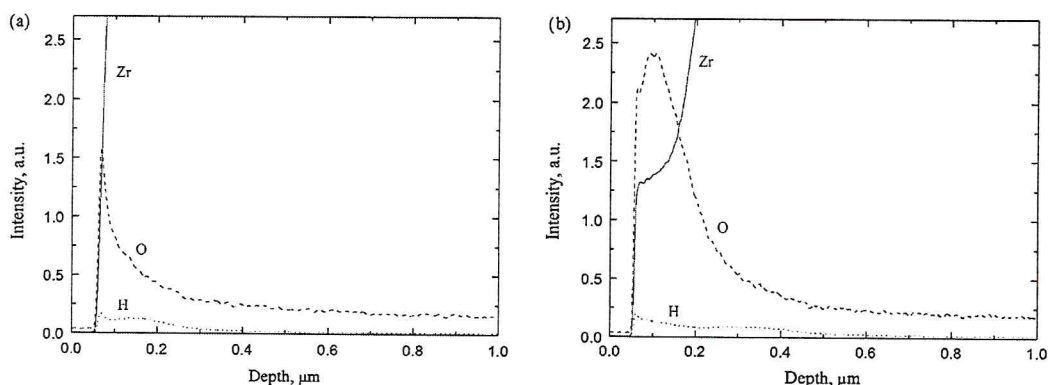**Fig. 1.** Microstructure of the Zr–1Nb surface before (a) and after (b) PEB.

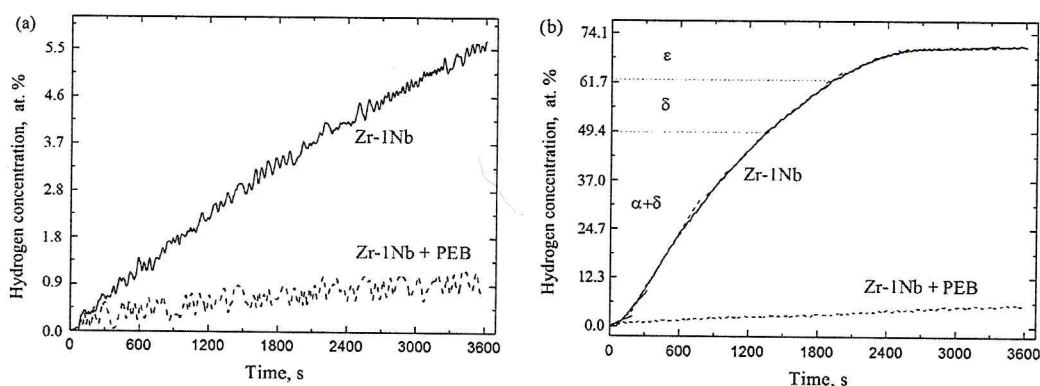Fig. 3. Elements' distribution in the zirconium alloy before and after PEB.

Fig. 4. Isotherms of Zr–1Nb alloy interaction with hydrogen at different temperatures: (a) –350 °C and (b) –450 °C.
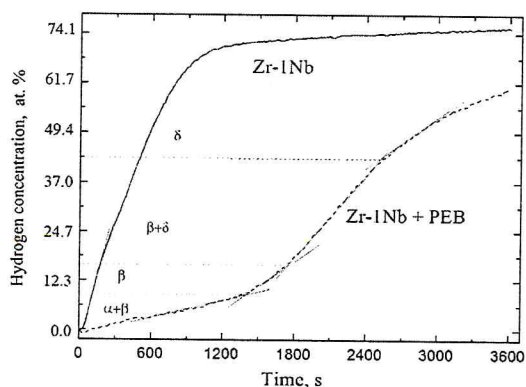
Fig. 5. Isotherms of Zr–1Nb alloy interaction with hydrogen at 550 °C.

Table 1
Hydrogen content in samples after saturation from gas atmosphere.

Samples	Hydrogen concentration, at.%
Initial + H (350 °C)	2.6 ± 0.3
PEB + H (350 °C)	0.7 ± 0.1
Initial + H (450 °C)	63.3 ± 6.3
PEB + H (450 °C)	3.1 ± 0.3
Initial + H (550 °C)	65.4 ± 6.5
PEB + H (550 °C)	54.0 ± 5.4

of (350–450) °C the hydrogen adsorption rate during the whole experiment does not change. Increasing the temperature leads to an increase in the rate of hydrogenation. At 550 °C the hydrogen diffusion rate changes is caused by the $\alpha \rightarrow (\alpha + \beta) \rightarrow (\beta + \delta) \rightarrow \delta$ phase transitions.

The increased of Zr–1Nb alloy to hydrogenation after the PEB treatment is confirmed by experimental results. Table 1 contains the data for hydrogen content in zirconium alloy after saturation in gas.

According to the investigation of elements' distribution profiles, the hydrogen penetrates deeper. There is an unusual distribution of hydrogen in the thin surface layer (less than 1 μm), see Fig. 6.

The hydrogenation of the initial alloy in gas results in a change of zirconium alloy lattice parameters and an increase of surface elastic stresses (Table 2). The analysis of the results demonstrates that the hydrogen is in the form of a hydride phase.

The Surface micrographs of the sample below, which was not treated by PEB and that was obtained by cooling from 450 °C to room temperature at a rate of 6 °C/min are zirconium δ-hydride (Figs. 7–9). These results are confirmed by XRD analysis. It is known that in hydrogenated zirconium after a specific deformation, the hydride plates break and microcracks occur. Unlike the initial samples the surface of samples treated by PEB after the saturation by hydrogen do not contain cracks and delamination of the material.

Thus, the cause of decrease adsorption by the treated surface of Zr–1Nb alloy appears to be the formation of a protective oxide film after PEB irradiation. It is known that during the interaction of hydrogen with a metal, the metal's surface condition is of great significance [5,16–19]. All hydride-forming metals, excluding palladium, have a greater affinity for oxygen than for hydrogen and are usually covered by an oxide film. Such films often serve as
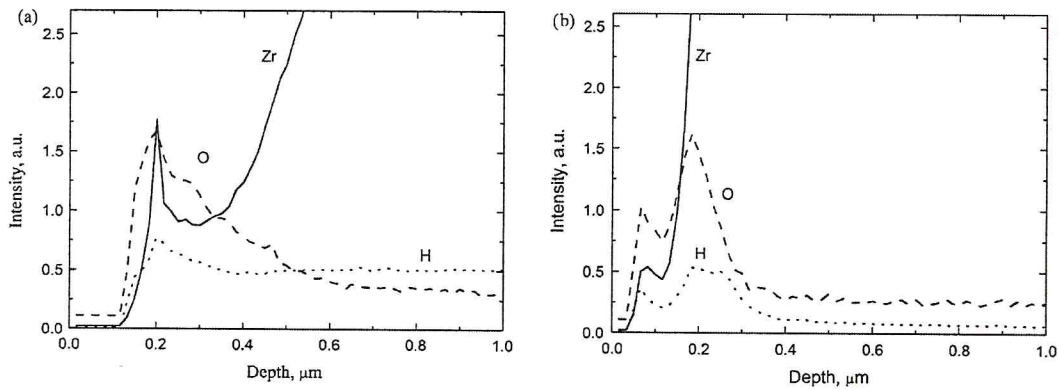
Fig. 6. The elements' distribution after saturation by hydrogen at 350 °C of initial (a) and treated (b) samples.

Table 2
Results of XRD analysis of zirconium alloy saturated by hydrogen in gas at 450 °C.

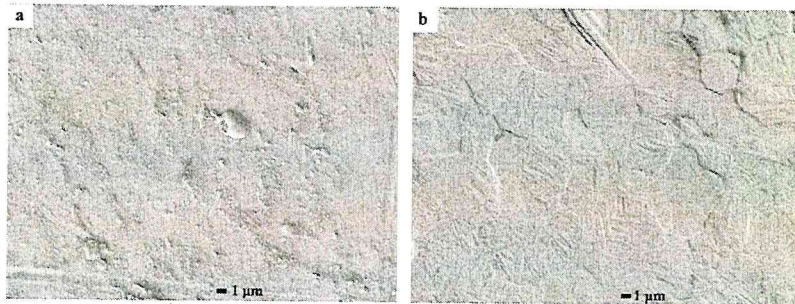| Samples	Phase	Phases content, vol.%	Lattice parameters, ±0.0005 Å	$\Delta d/d$, $\times 10^{-3} \pm 0.009 \times 10^{-3}$
Initial + H	Zr	62.4	$a = 3.2296$ $c = 5.1382$	0.2
	ZrH	0.3	$a = 4.6960$ $c = 5.0252$	–
	$ZrH_{1.5}$	36.1	$a = 4.7731$	1.1
	Zr_3O	1.2	$a = 5.6347$ $c = 5.1541$	0.5
PEB + H	Zr	61.9	$a = 3.2302$ $c = 5.1409$	0.6
	$ZrH_{1.5}$	25.9	$a = 4.7686$	–
	ZrH	2.8	$a = 4.4866$ $c = 4.8795$	5.7
	Zr_3O	8.4	$a = 5.6999$ $c = 5.1285$	3.1

Fig. 7. Zr–1Nb surface microstructure after saturation by hydrogen at $T = 350$ °C: (a) initial and (b) after PEB.

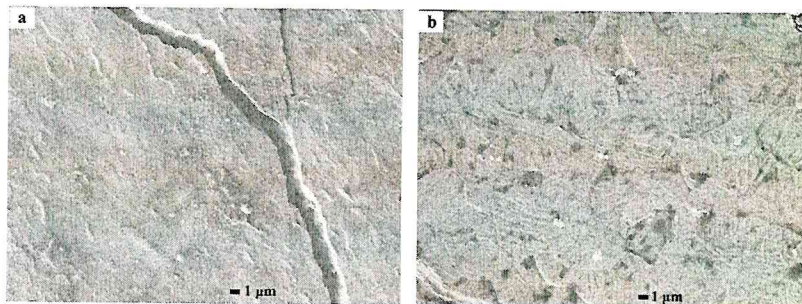**Fig. 8.** Zr–1Nb surface microstructure after saturation by hydrogen at $T = 450$ °C: (a) initial and (b) after PEB.

protective coatings from reacting gas penetration. For the initiation of hydrogen interaction with a metal these films are preliminarily disrupted or removed. For instance, the volume of the oxide on the surface of titanium or zirconium is "dissolved" and reduced (in the case of a massive sample) during heating in a vacuum or in a hydrogen atmosphere. The presence of an oxide layer on the zirconium
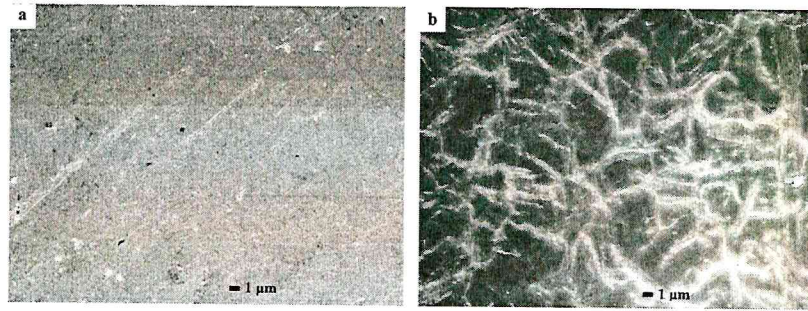
Fig. 9. Zr–1Nb surface microstructure after saturation by hydrogen at T = 550 °C: (a) initial and (b) after PEB.

alloy surface helps to significantly increase the activation energy of molecular hydrogen dissociation and, hence, requires additional higher temperatures to promote the reaction [20].

In particular, higher temperatures to promote the reaction is needed to insufficient mobility of oxygen (at 350–450 °C) because of the transformation of a regular α-zirconium face-centered close-packed lattice into a regular δ-hydride face-centered cubic structure. However, during hydrogenation at 550 °C and with a hydrogen concentration of greater than 7 at.%, the zirconium matrix experiences allotropic transformation (solid phase transformation of face-centered close-packed structure into a body-centered cubic lattice, i.e. "a regular- to irregular" transformation). As a result, the oxygen diffusion coefficient is equal its value in pure zirconium at temperatures higher than 1136 K.

5. Conclusion

The treatment of Zr–1Nb alloy with high-current pulsed electron beam results in a decrease of hydrogen amount absorbed by the sample during subsequent hydrogenation in gas at the temperature range of (350–550 °C). For the samples treated by PEB and saturated with hydrogen, the $C_{H\ initial}/C_{H\ treated}$ ratio was the following: at T = 350 °C $C_{H\ untreated}/C_{H\ treated}$ = 3.5; at T = 450 °C $C_{H\ untreated}/C_{H\ treated}$ = 20; at T = 550 °C–$C_{H\ untreated}/C_{H\ treated}$ = 1.2, respectively.

The decline in hydrogen sorption in treated Zr–1Nb alloy surface is primarily caused by the formation of a specific hardening structure under irradiation action at temperatures exceeding the melting temperature and the consequent high-speed surface cooling. The nanocrystalline structure has more boundaries that serve as effective traps for hydrogen. Consequently, the hydrogen accumulates and is retained in a thin layer in the material treated by PEB. On the other hand, the increase of hydrogen-resistance in treated samples is connected with the formation of a protective oxide film after PEB irradiation. This was confirmed by the results of a hydrogen depth distribution analysis in the samples and a subsequent investigation of the absolute hydrogen content in the bulk of the Zr–1Nb alloy. According to the investigation the oxide films formed after PEB irradiation temporarily protected the sample from hydrogenation. The oxide films are dissolved during interaction with hydrogen in non-oxygen atmosphere. The time before

the protective oxide is dissolved depends on the hydrogenation temperature and decreases with temperature increasing. Fast hydrogen sorption and subsequent hydride formation occurs after the protective oxide dissolving.

Acknowledgement

References

[1] J.-H. Huang, Metall. Mater. Trans. A 29 (1998) 1047–1056.
[2] Y.S. Kim, J. Alloys Comp. 453 (2008) 210–214.
[3] Y. Gou, Y. Li, H. Chen, Mater. Des. 30 (2009) 1231–1235.
[4] S.V. Ivanova, Int. J. Hydrogen Energy 27 (2002) 819–824.
[5] I.P. Chernov, N.S. Pushilina, E.V. Chernova, A.M. Lider, S.V. Ivanova, Tech. Phys. 58 (2013) 1280–1283.
[6] I.P. Chernov, S.V. Ivanova, K.V. Kryoning, N.N. Koval, V.V. Larionov, A.M. Lider, N.S. Pushilina, E.N. Stepanova, O.M. Stepanova, Y.P. Cherdantsev, Tech. Phys. 57 (2012) 392–398.
[7] I.P. Chernov, Y.P. Cherdantsev, A.M. Lider, Y.I. Tyurin, N.S. Pushilina, S.V. Ivanova, J. Surf. Invest. 4 (2010) 255–261.
[8] A.D. Pogrebnjak, D.I. Proskurovskii, Phys. Status Solidi A 145 (1994) 9–49.
[9] V.P. Rotshtein, Yu.F. Ivanov, A.B. Markov, D.I. Proskurovsky, K.V. Karlik, K.V. Oskomov, B.V. Uglov, A.K. Kuleshov, M.V. Novitskaya, S.N. Dub, Y. Pauleau, I.A. Shulepov, Surf. Coat. Technol. 22 (2006) 6378–6383.
[10] B. Gao, S. Hao, J. Zou, W. Wu, C. Dong, Surf. Coat. Technol. 201 (2007) 6297–6303.
[11] C. Dong, A.M. Wu, S.Z. Hao, et al., Surf. Coat. Technol. 163–164 (2003) 620–624.
[12] D.I. Proskurovsky, V.P. Rotshtein, G.E. Ozur, Yu.F. Ivamov, A.B. Markov, J. Surf. Coat. Technol. 125 (2000) 49–56.
[13] D.I. Proskurovsky, V.P. Rotshtein, G.E. Ozur, A.B. Markov, D.S. Nazarov, J. Vac. Sci. Technol. A 16 (4) (1998) 2480–2488.
[14] V. Rotshtein, Yu. Ivanov, A. Markov, Surface treatment of materials with lowenergy, high-current electron beams, in: Y. Pauleau (Ed.), Book Materials Surface Processing by Directed Energy Techniques, vol. 763, 2006, pp. 205–240.
[15] V.N. Kudiiarov, L.V. Gulidova, A.M. Lider, N.S. Pushilina, Adv. Mater. Res. 740 (2013) 690–693.
[16] M. Steinbruck, J. Nucl. Mater. 334 (2004) 58–64.
[17] Andrzej. Zielinski, Sylwia. Sobieszczyk, Int. J. Hydrogen Energy 36 (2011) 8619–8629.
[18] Darren Broom, Hydrogen storage materials. The characterization of their storage properties. 2011, XII, 260p, Hardcover. ISBN: 978-0-85729-220-9.
[19] K.A. Terrani, M. Balooch, D. Wongsawaeng, S. Jaiyen, D.R. Olander, J. Nucl. Mater. 397 (2010) 61–68.
[20] Doonyapong Wongsawaeng, Sarawut Jaiyen, J. Nucl. Mater. 403 (2010) 19–24.